to be made. The difference between human or bovine insulin or even the presence of one genetic error in its 51 amino acid structure can *now* be detected by mass spectrometry. The insulin work gives encouragement that higher molecular weight proteins will give interpretable mass spectra. If one were able to determine the molecular weight of an unknown protein in the 10 000 to 20 000 range *prior* to sequence analysis, one would then be in a position to design a more efficient protocol for its sequence determination.

To extend these methods to higher molecular weights, the size of the molecule relative to the area of excitation will eventually become an important consideration. The chemically protected oligonucleotides are a convenient molecular gauge to study this question since each residue is ~0.5 nm long and the protecting groups foster a linear tertiary structure. The largest studied thus far by ^{252}Cf PDMS is a 14-mer, a 7-nm-long molecule with the same long dimension as hemoglobin, which is a medium-sized globular protein with a molecular weight of approximately 65 000. Whether science would be enlightened by knowing the molecular weight of hemoglobin more accurately is not immediately obvious. Perhaps these kinds of measurements would provide answers for which there are no questions. Nevertheless the history of molecular biology has demonstrated that higher resolution generally leads to deeper levels of understanding.

So, if these be the goals of particle-induced desorption mass spectrometry, the space yet to be covered includes energy transport in molecular solids, surface chemistry in the high-energy–short-time domain, and the dynamics of surface-ionization desorption for large organic molecules—the fundamental ingredients of the process, which, considered separately, constitute interesting fundamental studies in physics and chemistry.

I am particularly grateful to Professor A. Benninghoven, Dr. Fred Saalfeld, and Dr. Bo Sundqvist, who recently organized and hosted very timely and effective workshops on this subject. I am indebted to my "in-house" colleagues, D. F. Torgerson, C. J. McNeal, R. A. Martin, T. Bickford, D. Shelton, and M. Bailey, who have dedicated considerable effort to creating and sustaining the ^{252}Cf PDMS work. The financial support of the National Science Foundation (Grant CHE-79-04863), the National Institutes of Health (GM26096), and the Robert A. Welch Foundation (Grant A-258) is gratefully acknowledged.

Nuclear, Electronic, and Frequency Factors in Electron-Transfer Reactions

NORMAN SUTIN

Department of Chemistry, Brookhaven National Laboratory, Upton, New York 11973

Received December 3, 1981

Electron-transfer reactions are distinguished by their ubiquity and by their essential roles in many physical, chemical, and biological processes. Thus, understanding the factors which determine electron-transfer rates is of considerable importance.

Although a number of theories have been proposed,[1-15] there is general agreement that the crux of the electron-transfer problem is the fact that the equilibrium nuclear configuration of a species changes when it gains or loses an electron. In the case of a metal complex this configuration change involves changes in the metal–ligand and intraligand bond lengths and angles as well as changes in the vibrations and rotations of the surrounding solvent dipoles.

These configuration changes are similar to those that result from the electronic redistribution that occurs when a molecule absorbs or emits a photon. In view of the similarity of the nuclear configuration changes resulting from electron transfer and photon capture (or emission), and, more importantly, because the two processes occur rapidly on the nuclear time scale, the rates of thermal electron transfer, electronic energy transfer, and a variety of nonradiative processes can be understood in terms of a common theoretical framework.[15] Within this framework the rate constants can be expressed as a product of a nuclear, an electronic, and a frequency factor.

Norman Sutin received his Ph.D. degree from Cambridge University in 1953. From 1954 to 1955 he was a postdoctoral research fellow at Durham University, Durham, England. In 1956 he joined the Chemistry Department at Brookhaven National Laboratory, where he is now a Senior Chemist. He has been an affiliate of Rockefeller University, New York, and has held visiting professorships at the State University of New York at Stony Brook, at Columbia University, and at Tel Aviv University.

(1) (a) Marcus, R. A. *Annu. Rev. Phys. Chem.* **1964**, *15*, 155. (b) Marcus, R. A. *J. Chem. Phys.* **1965**, *43*, 679.
(2) (a) Marcus, R. A. *Discuss. Faraday Soc.* **1960**, *29*, 21. (b) Marcus, R. A. *Int. J. Chem. Kinet.* **1981**, *13*, 865.
(3) Hush, N. S. *Trans. Faraday Soc.* **1961**, *57*, 557.
(4) Hush, N. S. *Electrochim. Acta* **1968**, *13*, 1005.
(5) Sutin, N. *Annu. Rev. Nucl. Sci.* **1962**, *12*, 285.
(6) Dogonadze, R. R.; Kuznetsov, A. M.; Levich, V. G. *Electrochim. Acta* **1968**, *13*, 1025.
(7) Dogonadze, R. R. In "Reactions of Molecules at Electrodes"; Hush, N. S., Ed.; Wiley-Interscience: New York, 1971; Chapter 3, p 135.
(8) Kestner, R. N.; Logan, J.; Jortner, J. *J. Phys. Chem.* **1974**, *78*, 2148.
(9) Ulstrup, J.; Jortner, J. *J. Chem. Phys.* **1975**, *63*, 4358.
(10) Van Duyne, R. P.; Fischer, S. F. *Chem. Phys.* **1974**, *5*, 183.
(11) German, E. D.; Dvali, V. G., Dogonadze, R. R.; Kuznetsov, A. M. *Elektrokhimiya* **1976**, *12*, 639.
(12) Efrima, S.; Bixon, M. *Chem. Phys.* **1976**, *13*, 447.
(13) Change, B.; DeVault, D. C.; Frauenfelder, H.; Marcus, R. A.; Schrieffer, J. B.; Sutin, N. Eds. "Tunneling in Biological Systems"; Academic Press: New York, 1979.
(14) Ulstrup, J. "Charge Transfer Processes in Condensed Media"; Springer-Verlag: West Berlin, 1979.
(15) Jortner, J.; *Philos. Mag.* **1979**, *40*, 317.

0001-4842/82/0115-0275$01.25/0

Formation of the Precursor Complex

The nuclear and electronic factors both become more favorable with decreasing separation of the reactants. Consequently the first step in a bimolecular-electron-transfer reaction in solution is the diffusion together of the separated reactants to form a precursor complex. This is followed by electron transfer within the precursor complex to form a successor complex.

$$ML_m^{2+} + NL_n^{3+} \rightleftharpoons ML_m^{2+}\cdots NL_n^{3+}$$

$$ML_m^{2+}\cdots NL_n^{3+} \rightarrow ML_m^{3+}\cdots NL_n^{2+}$$

Opposing the close approach of the reactants is the Coulombic work required to bring together similarly charged reactants and ultimately the electron–electron repulsions. Different systems will reflect different compromises between these opposing factors. If two reactants can increase their electronic coupling by squeezing together so that their inner-coordination shells interpenetrate, they will do so to the extent that the increase in the electronic factor is not offset by the work required to achieve the improved electronic interaction.

We do explore this aspect here; instead we use a model in which it is assumed that most of the contribution to the rate comes from reaction at separation distances between r and $r + \delta r$ where $r \geq \sigma$, the sum of the radii of the reactants. Under these conditions the rate constant for the reaction is given by[16-20]

$$\frac{1}{k_{obsd}} = \frac{1}{k_{diff}} + \frac{1}{k_{act}} \quad (1)$$

$$k_{act} = K_A(r)k_{el}(r) \quad (2)$$

$$K_A(r) = \frac{4\pi N r^2 \delta r}{1000} \exp\left(-\frac{w(r)}{RT}\right) \quad (3)$$

$$k_{el}(r) = \nu_n(r)\kappa_{el}(r)\kappa_n(r) \quad (4)$$

where k_{diff} is the diffusion-controlled rate constant for the formation of the precursor complex from the separated reactants, k_{act} is the activation-controlled rate constant for the bimolecular reaction, $K_A(r)$ is the equilibrium constant for the formation of reactant pairs separated by a distance between r and $r + \delta r$, $w(r)$ is the work required to bring the reactants to the separation distance r, $k_{el}(r)$ is the first-order rate constant for electron transfer at the distance r, $\nu_n(r)$ is an effective nuclear frequency, $\kappa_n(r)$ is the nuclear factor, and $\kappa_{el}(r)$ is the electronic factor. The magnitudes of the nuclear and electronic factors range from zero to unity; $\kappa_n = 1$ for a barrierless reaction, and $\kappa_{el} = 1$ when the electronic interaction of the reactants is sufficiently large. $K_A(r)\nu_n(r)$ and $\nu_n(r)$ are the frequency factors for bimolecular and unimolecular reactions, respectively. For unimolecular reactions the rate constant is simply equal to $\nu_n\kappa_{el}\kappa_n$.

(16) Brunschwig, B. S.; Logan, J.; Newton, M. D.; Sutin, N. *J. Am. Chem. Soc.* **1980**, *102*, 5798.
(17) Brown, G. M.; Sutin, N. *J. Am. Chem. Soc.* **1979**, *101*, 883.
(18) (a) Sutin, N. In "Inorganic Reactions and Methods"; Zuckerman, J. J., Ed.; Springer-Verlag: West Berlin, in press. (b) Sutin, N. In "Bioinorganic Chemistry"; Eichhorn, G. L., Ed.; American Elsevier: New York, 1973; Vol. 2, Chapter 19, p 611.
(19) (a) Sutin, N.; Brunschwig, B. S. *ACS Symp. Ser.* **1982**, *No. 198*, 105. (b) Sutin, N. *Prog. Inorg. Chem. 30*, in press.
(20) Equations 1–4 are equivalent to certain equations introduced by Marcus.[2]

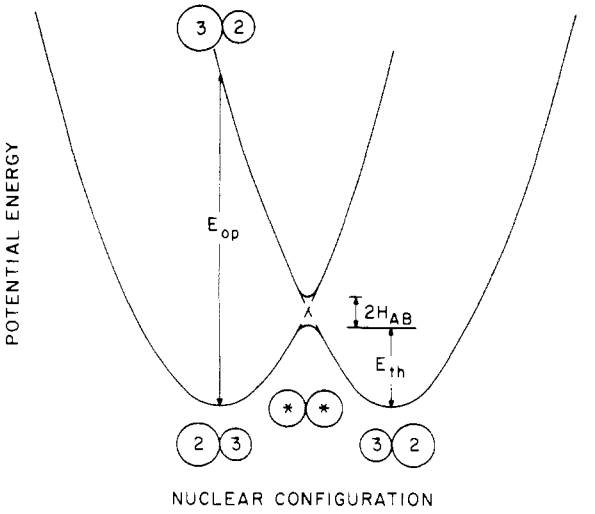

Figure 1. Plot of the potential energy of the reactants (precursor complex) and products (successor complex) as a function of nuclear configuration for an electron-exchange reaction. E_{th} is the barrier for the thermal electron transfer, E_{op} is the energy for the light-induced electron transfer, and the splitting at the intersection of the surfaces is equal to $2H_{AB}$ where H_{AB} is the electronic coupling matrix element. Note that $H_{AB} << E_{th}$ in the weak interaction model. The circles indicate the relative nuclear configurations of the two reactants of charges 2+ and 3+ in the precursor complex, the optically excited precursor complex, the activated complex, and the successor complex.

Work Terms. In general the work required to bring the reactants to the separation distance r includes both Coulombic and non-Coulombic (hydrophobic) contributions. If the work is prediminantly Coulombic and the reactants are spherical, then $w(r)$ is given by[21]

$$w(r) = \frac{z_2 z_3 e^2}{2D_s r}\left(\frac{\exp(\beta\sigma_2\mu^{1/2})}{1+\beta\sigma_2\mu^{1/2}} + \frac{\exp(\beta\sigma_3\mu^{1/2})}{1+\beta\sigma_3\mu^{1/2}}\right)\exp(-\beta r\mu^{1/2}) \quad (5)$$

where $\beta = (8\pi N e^2/1000 D_s kT)^{1/2}$, z_2 and z_3 are the charges on the two reactants, σ_2 (or σ_3) is equal to the radius of the reactant a_2 (or a_3) plus the radius of the main ion of opposite charge in the reactant's ion atmosphere, and D_s is the static dielectric constant of the medium. Note that eq 5 reduces to the familiar eq 6

$$w(\sigma) = \frac{z_2 z_3 e^2}{D_s\sigma(1+\beta\sigma\mu^{1/2})} \quad (6)$$

when $r = \sigma = (a_2 + a_3)$ and the radii of all the ions are equal. Although more complex expressions for the work required to form the precursor complex are available,[22] the above expressions are adequate for the present purpose.

The Nuclear Factor

The fitness of a particular nuclear configuration for electron transfer is determined by energy and momentum conservation requirements. Since internuclear distances and nuclear velocities do not change during an electronic transition (Franck–Condon principle), the actual electron transfer occurs at essentially constant

(21) (a) Debye, P. *Trans. Electrochem. Soc.* **1942**, *82*, 265. (b) The bimolecular reactions that are considered involve electron transfer between metal centers of formal charge 2+ and 3+ and subscript 2 or 3 denotes the charge on the metal center under consideration.
(22) Friedman, H. L. *Pure App. Chem.* **1981**, *53*, 1277.

nuclear configuration and momentum.

This requirement is incorporated into classical electron-transfer theories by postulating that the electron transfer occurs at the intersection of the reactants' (precursor complex) and products' (successor complex) potential energy surfaces. A profile of two such intersecting surfaces is shown in Figure 1 for an electron-transfer reaction in which no net chemical change occurs (an electron-exchange reaction).[1-5] The Franck–Condon principle is obeyed since the nuclear configurations and energies of the reactants and products are the same at the intersection (activated complex).

In quantum-mechanical theories, on the other hand, the intersection of the potential energy surfaces is deemphasized, nuclear tunneling from the initial to the final state is allowed for, and the appropriateness of a nuclear configuration for electron transfer is related to the square of the overlap of the vibrational wave functions of the reactants and products (i.e., to the Franck–Condon factors for the transition).[6-16]

The nuclear configuration changes depicted in Figure 1 involve both the inner and the outer (solvent) coordination shells of the reactants and products and are conveniently discussed in terms of the reorganization parameters λ_{out} and λ_{in} defined by [1-5]

$$\lambda_{out} = (\Delta e)^2\left(\frac{1}{2a_2} + \frac{1}{2a_3} - \frac{1}{r}\right)\left(\frac{1}{D_{op}} - \frac{1}{D_s}\right) \quad (7)$$

$$\lambda_{in} = \tfrac{1}{2}\Sigma f_i(d_2^\circ - d_3^\circ)_i^2 \quad (8)$$

or the corresponding free energies, defined by $\Delta G_{out}^* = \lambda_{out}/4$ and $\Delta G_{in}^* = \lambda_{in}/4$. In these expressions D_{op} is the optical dielectric constant of the medium (equal to the square of the refractive index), $f_i = 2f_2f_3/(f_2 + f_3)$ is a reduced force constant for the ith inner-sphere vibration, $(d_2^\circ - d_3^\circ)_i$ is the corresponding difference in the equilibrium bond distances in the two oxidation states, and the summation is over *all* the intramolecular vibrations. The expressions for λ_{out} and λ_{in} are based upon a dielectric continuum model for the solvent and a harmonic oscillator model for the inner-sphere vibrations, respectively. These equations have occasionally been misinterpreted in the literature; in the usual generalized valence force field there are both diagonal and off-diagonal force constants, and sometimes only the diagonal ones have been introduced into eq 8. However, as has been stressed,[2] the constants to be introduced into eq 8 are the "normal mode force constants".

Classical Expressions. In the high-temperature limit the reaction proceeds classically: the system acquires the nuclear configuration appropriate to the intersection region and the nuclear factor is given by [16-19]

$$\kappa_n = \exp(-\Delta G^*/RT) \quad (9)$$

where[1,2]

$$\Delta G^* = \frac{\lambda}{4}\left(1 + \frac{\Delta G_{AB}^\circ}{\lambda}\right)^2 \quad (10)$$

In the above expressions ΔG^* is the classical free-energy barrier to the reaction (and does *not* include the work required to bring the reactants together), $\lambda = (\lambda_{in} + \lambda_{out})$, ΔG_{AB}° is the free-energy change for the reaction at the separation distance r (and is related to ΔG°, the free-energy change when the two reactants and products are an infinite distance apart, by $\Delta G_{AB}^\circ = \Delta G^\circ - \Delta G_A^\circ + \Delta G_B^\circ$, where ΔG_A° and ΔG_B° are the free energies of formation of the precursor and successor complexes, respectively), and the splitting at the intersection of the surfaces has been neglected.

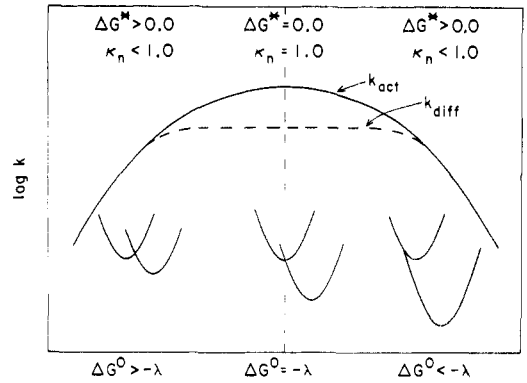

Figure 2. Plot of the logarithm of the activation-controlled and diffusion-limited rate constants as a function of increasing driving force in the classical model. The normal free-energy region, $\Delta G^\circ > -\lambda$, is on the left, and the inverted free-energy region, $\Delta G^\circ < -\lambda$, is on the right. The three pairs of intersecting curves illustrate the reactants' and products' energy surfaces in the normal, barrierless, and inverted regions; κ_n is the nuclear factor ΔG^* the activation energy associated with the nuclear configuration change, and λ is the reorganization parameter. The dashed horizontal curve is for a diffusion-controlled reaction and the case illustrated is for $k_{act} > k_{diff}$ when $\Delta G^\circ \sim -\lambda$; under these conditions the observed rate constant will be equal to k_{diff}. Note that k_{act} may be less than k_{diff} when $\Delta G^\circ \sim -\lambda$ if the electronic factor is very small; under these conditions the observed bimolecular rate constant will be equal to k_{act}. For unimolecular reactions the observed rate constant is always equal to k_{act}.

For many purposes it is convenient to distinguish two free-energy regions depending on the magnitude of $\Delta G_{AB}^\circ/\lambda$.[1,2] The first is called the normal free-energy region and is defined by $-\lambda < \Delta G_{AB}^\circ < \lambda$. In this region ΔG^* decreases and κ_n increases as λ or ΔG_{AB}° decreases. When $\Delta G_{AB}^\circ = -\lambda$, $\Delta G^* = 0$ and the reaction is barrierless. Under these conditions $\kappa_n = 1$ and the observed rate constant is equal to the smaller of k_{diff} and $K_A\kappa_{el}\nu_n$.[19b] The second region is called the abnormal or inverted free-energy region and is defined by $\Delta G_{AB}^\circ < -\lambda$.[1,2] In this region ΔG^* increases and κ_n decreases as λ decreases or ΔG_{AB}° becomes more negative. These cases are illustrated in Figure 2.

Quantum-Mechanical Expressions. The above expressions are derived from classical activated-complex theory and can be considered as the high-temperature limits of quantum-mechanical expressions. At lower temperatures or higher frequencies ($h\nu > kT$) the above expressions must be corrected for quantum-mechanical effects. Such corrections can be considerable and, as mentioned earlier, are usually made by introducing Franck–Condon factors for the transition. The corrections are more important for the inner-sphere modes since their frequencies are higher (300–3000 cm^{-1}) than the average frequency associated with the solvent reorganization (~30 cm^{-1} for water).[16] The quantum-mechanical expressions for two low-temperature cases are of interest. These are special cases of the normal and inverted regions mentioned above.

(1) $\Delta G_{AB}^\circ \sim 0$. Under these conditions the relative vertical displacement of the energy surfaces is small and the nuclear factor is given by[16,23]

$$\kappa_n = \exp\left[-\left(E_{out} + E_{in}\left(\frac{4kT}{h\nu_{in}}\right)\tanh\left(\frac{h\nu_{in}}{4kT}\right)\right)/4RT\right] \quad (11)$$

where ν_{in} is an average inner-sphere frequency, and E_{out} and E_{in} are solvent and inner-sphere reorganization parameters (vide infra). More generally, the second term in the exponent should be replaced by a sum over *all* the inner-sphere vibrations ranging from, at the low frequency limit, the metal–ligand stretching vibrations (300–500 cm^{-1}) and, at the high frequency limit, the C–H and N–H stretching vibrations of the ligands ($\sim$ 3000 cm^{-1}). Of course, at sufficiently low temperatures the solvent reorganization should also be treated quantum mechanically.

(2) $\lambda << -\Delta G_{AB}°$. Under these conditions the relative horizontal displacement of the energy surfaces is small. Provided that $E_\lambda \leq h\langle\nu\rangle$, where $\langle\nu\rangle$ is the mean vibrational frequency, eq 12 for the nuclear factor can be

$$\kappa_n = \exp\left(\frac{\gamma\Delta E}{h\nu_M} - \frac{E_M}{h\langle\nu\rangle}\right) \quad (12)$$

derived from the Englman–Jortner equations.[24] In eq 12, $\gamma = (\ln(-\Delta E/E_M) - 1)$ is positive, ΔE is the electronic energy difference between the final and initial states (and is negative), ν_M is the maximum frequency of the affected modes, E_M is the contribution of the maximum frequency modes to $E_\lambda = \sum E_i$, and it is assumed that all the E_i and ν_i are similar.

Equation 12 is a statement of the energy-gap law of radiationless transition theory. According to this law the transition probability in the weak coupling limit varies exponentially with the energy gap.[24] Although it is only valid in the low-temperature limit (where the rate constants have become temperature independent), room temperature can be regarded as in the low-temperature regime provided that the relevant frequencies are sufficiently high. The exponential dependence of the transition probability on the first power of the energy difference predicted by the energy-gap law should be contrasted with the dependence on the second power of the energy difference predicted by the classical theory.

The above expressions are written in terms of energies rather than free energies in order to emphasize their quantum-mechanical origin. In practice, E_{out} is usually replaced by λ_{out}, E_{in} by λ_{in}, E_λ by λ, and ΔE by $\Delta G_{AB}°$.

Applications. The magnitudes of the nuclear factors for various electron-transfer processes are presented in Table I. This table includes values of κ_n for unimolecular processes such as spin conversion, the radiationless decay of excited states, and electron transfer in mixed-valence (bridged) systems, as well as κ_n values for bimolecular reactions. It will be seen that the nuclear factors span a very wide range, from $\sim 10^{-14}$ to $\sim 10^{-1}$, reflecting the variations in E_λ and $\Delta E/E_\lambda$ and the assumptions made for ν_M.

The first two entries in Table I are for spin equilibrium systems of the type

$$\text{low spin} \rightleftharpoons \text{high spin}$$

which have been studied by temperature-jump and ultrasonic relaxation techniques.[25,28,36,37] Since the formation of the high-spin state of the complex involves the population of $d\sigma^*$ orbitals, the nuclear configuration changes accompanying the spin conversion are generally large—the metal–ligand bond changes are typically 0.11–0.15 Å,[27,28] although larger bond changes have also been reported.[25,38] Furthermore, the equilibrium constant for the spin interconversion is $\sim$1. Consequently, the spin-conversion processes lie in the normal free-energy region of classical activated-complex theory.[39]

When the two spin states differ considerably in their stabilities, they are considered as the ground and excited states of the complex.[40] Under these conditions the excited state can be generated by optical (or chemical) pumping and the spin relaxation is viewed as an excited-state decay. If the excited state emits, then the nuclear factor for the transition can be calculated by using the appropriate Stokes shift ($E_\lambda = E_s/2$).[41] In contrast to the spin-equilibrium processes, the excited-state decays are accompanied by relatively large energy changes; consequently they generally occur in the inverted free-energy region of activated-complex theory.[39]

Of the systems in Table I, the conversion of the ligand-field (LF) excited state of $Fe(bpy)_3^{2+}$ to the ground state is essentially a barrierless process. On the other hand, the decay of the metal-to-ligand charge-transfer (MLCT) excited state of $Ru(bpy)_3^{2+}$ takes place in the highly inverted region, and this is responsible for the much lower nuclear factor calculated for this transition ($\kappa_n \sim 10^{-10}$ for $h\nu_M = 1.3 \times 10^3$ cm^{-1};[42,43] see Table I,

(23) Holstein, T. In "Tunneling in Biological Systems"; Chance, B., DeVault, D. C., Frauenfelder, H., Marcus, R. A., Schrieffer, J. B., Sutin, N., Eds.; Academic Press: New York, 1979.

(24) (a) Englman, R.; Jortner, J. *Mol. Phys.* **1970**, *18*, 145. (b) Alternative expressions for the weak coupling limit are available.[9,10,24c] (c) Jortner, J. *J. Am. Chem. Soc.* **1980**, *102*, 6676. (d) Kestner, R. N.; Webman, I. *J. Phys. Chem.* **1979**, *83*, 451.

(25) Dose, E. V.; Hoselton, M. A.; Sutin, N.; Tweedle, M. F.; Wilson, L. J. *J. Am. Chem. Soc.* **1978**, *100*, 1141.

(26) Creutz, C.; Chou, M.; Netzel, T. L.; Okumura, M.; Sutin, N. *J. Am. Chem. Soc.* **1980**, *102*, 1309.

(27) Albertsson, A.; Oskarsson, A.; Stahl, K.; Svensson, C.; Ymen, I. *Acta Crystallogr., Sect. B* **1981**, *B37*, 50.

(28) Binstead, R. A.; Beattie, J. K.; Dewey, T. G.; Turner, D. H. *J. Am. Chem. Soc.* **1980**, *102*, 6442.

(29) Sutin, N.; Creutz, C. *Pure Appl. Chem.* **1980**, *52*, 2717.

(30) Creutz, C. *Inorg. Chem.* **1978**, *17*, 3723.

(31) Sutton, J. E.; Sutton, P. M.; Taube, H. *Inorg. Chem.* **1979**, *18*, 1017.

(32) Rieder, K.; Taube, H. *J. Am. Chem. Soc.* **1977**, *99*, 7891.

(33) Sutton, J. E.; Taube, H. *Inorg. Chem.* **1981**, *20*, 3125.

(34) Geselowitz, D.; Taube, H. to be published.

(35) Hair, N. J.; Beattie, J. K. *Inorg. Chem.* **1977**, *16*, 245.

(36) Beattie, J. K.; Sutin, N.; Turner, D. H.; Flynn, G. W. *J. Am. Chem. Soc.* **1973**, *95*, 2052. Beattie, J. K., Binstead, R. A.; West, R. J. *J. Am. Chem. Soc.* **1978**, *100*, 3044.

(37) Binstead, R. A.; Beattie, J. K.; Dose, E. V.; Tweedle, M. F.; Wilson, L. J. *J. Am. Chem. Soc.* **1978**, *100*, 5609.

(38) Churchill, M. R.; Gold, K.; Maw, C. E. Jr. *Inorg. Chem.* 1970, *9*, 1597.

(39) The normal free-energy region of activated-complex theory corresponds to the very strong coupling case of radiationless transition theory, while the inverted free-energy region of activated complex theory includes both the weak and strong coupling cases of radiationless transition theory.

(40) Alternatively, a spin equilibrium may be viewed as a system in which an electronically excited state is thermally populated.

(41) The Stokes shift is the difference between the energies of the absorption and emission maxima for a particular transition.

(42) (a) Klassen, D. M.; Crosby, G. A. *J. Chem. Phys.* **1968**, *48*, 1853. (b) Caspar, J. V.; Kober, E. M.; Sullivan, B. P.; Meyer, T. J. *J. Am. Chem. Soc.* **1982**, *104*, 630.

Table I
Nuclear and Frequency Factors for Electron-Transfer Reactions[a]

reaction	$10^{-3}E_\lambda$, cm^{-1}	$-10^{-3}\Delta E$, cm^{-1}	κ_n	ν_n, s^{-1} or $K_A\nu_n$, $M^{-1}\,s^{-1}$	ref
$FeL_6^{2+}(^1A) \rightleftharpoons FeL_6^{2+}(^5T)$ $(d\pi)^6 \quad (d\pi)^4(d\sigma^*)^2$	3.0-5.5[b]	~0	$(10^{-3}$-$10^{-2})$[e]	10^{13}	25, 26
$FeL_6^{3+}(^2T) \rightleftharpoons FeL_6^{3+}(^6A)$ $(d\pi)^5 \quad (d\pi)^3(d\sigma^*)^2$	4.8-9.0[c]	~0	$(10^{-3}$-$10^{-2})$[e]	10^{13}	25, 27, 28
$*Fe(bpy)_3^{2+}(^5T) \rightarrow Fe(bpy)_3^{2+}(^1A)$ $(d\pi)^4(d\sigma^*)^2 \quad (d\sigma)^6$	4.8[d]	7.3	10^{-1} [f]	10^{13}	26, 29
$*Ru(bpy)_3^{2+}(^3(d\text{-}\pi^*)) \rightarrow Ru(bpy)_3^{2+}(^1A)$ $(d\pi)^5(L\pi)^1 \quad (d\pi)^6$	0.80[g]	16.9	10^{-17}[e] 10^{-12} [h]	10^{13}	29
$(NH_3)_5Ru^{II}(4,4'\text{-bpy})Ru^{III}(NH_3)_5 \rightarrow$ $(NH_3)_5Ru^{III}(4,4'\text{-bpy})Ru^{II}(NH_3)_5$[n]	9.7	0	10^{-5} [e]	10^{12}	30, 31
$(NH_3)_5Ru^{II}(py)CH_2(py)Ru^{III}(NH_3)_5 \rightarrow$ $(NH_3)_5Ru^{III}(py)CH_2(py)Ru^{II}(NH_3)_5$[o]	12.4	0	10^{-7} [e]	10^{12}	32, 33
$Co(en)_3^{2+} + Co(en)_3^{3+} \rightarrow$ $Co(en)_3^{3+} + Co(en)_3^{2+}$	27.0[k]	0	10^{-14} [i]	10^{12}	18, 34
$Fe(H_2O)_6^{2+} + Fe(H_2O)_6^{3+} \rightarrow$ $Fe(H_2O)_6^{3+} + Fe(H_2O)_6^{2+}$	20.4[l]	0	10^{-11} [e]	10^{11}	19, 35
$Ru(bpy)_3^{2+} + Ru(bpy)_3^{3+} \rightarrow$ $Ru(bpy)_3^{3+} + Ru(bpy)_3^{2+}$	4.6	0	10^{-4} [e]	10^{12}	19
$Fe(H_2O)_6^{2+} + Ru(bpy)_3^{3+} \rightarrow$ $Fe(H_2O)_6^{3+} + Ru(bpy)_3^{2+}$	12.5[m]	4.7	10^{-3} [e]	10^{12}	19, 29
$*Ru(bpy)_3^{2+} + Ru(bpy)_3^{3+} \rightarrow$ $Ru(bpy)_3^{3+} + Ru(bpy)_3^{2+}$	5.2[m]	16.9	10^{-14},[e] 10^{-12} [j]	10^{12}	19, 29

[a] $E_\lambda = (E_{out} + E_{in})$. For the bimolecular reactions E_{out} was calculated by assuming that the separation distance of the reactants was equal to the sum of their van der Waals radii. Only symmetric breathing motions and changes in the metal-ligand distances have been considered in calculating E_{in}. The frequency factor is ν_n for unimolecular reactions and $K_A\nu_n$ for bimolecular reactions. [b] Based on metal-ligand bond length changes of 0.11-0.15 Å and $\nu_{in} = 390\ cm^{-1}$. [c] Based on metal-ligand bond length changes of 0.11-0.15 Å and $\nu_{in} = 450\ cm^{-1}$. [d] Based on metal-ligand bond length changes of 0.14 Å and $\nu_{in} = 390\ cm^{-1}$. [e] Calculated from eq 9. [f] Calculated using eq 4 of ref 23 with $\nu_o = 390\ cm^{-1}$. [g] This is an upper limit based on a Stokes shift of ≤ 0.2 eV.[29] [h] Calculated by using eq 12 with $E_M = 800\ cm^{-1}$ and $h\nu_M = 1.3 \times 10^3\ cm^{-1}$, which is the frequency of the vibrational progression seen in the emission spectrum of $Ru(bpy)_3^{2+}$.[42] The nuclear factor increases if higher values of E_M or $h\nu_M$ are used. Thus $\kappa_n = 10^{-10}$ if a value of $1.6 \times 10^3\ cm^{-1}$ is used for $h\nu_M$.[43] The presence of a C-H/C-D isotope effect on the lifetime of the excited state indicates some participation of the C-H stretching modes. [i] Calculated by using eq 11. [j] Calculated by using eq 12 with $E_M = 800\ cm^{-1}$ and $h\nu_M = 1.3 \times 10^3\ cm^{-1}$. [k] Based on metal-ligand bond length changes of 0.21 Å and $\nu_{in} = 409\ cm^{-1}$. [l] Based on metal-ligand bond length changes of 0.14 Å and $\nu_{in} = 432\ cm^{-1}$. [m] E_λ calculated from eq 13. [n] 4,4'-bpy = 4,4'-bipyridine. [o] $(py)CH_2(py)$ = 4,4'-methylenebis(pyridine).

footnote *h*). Note that the value of κ_n calculated from the classical expression (eq 9 and 10) is too low by very many orders of magnitude. The values of E_λ for the mixed-valence systems were calculated from the energies of the intervalence band maxima ($E_\lambda = E_{op}$ when $\Delta E = 0$) and arise primarily from the solvent barrier.

We next consider the nuclear factors for bimolecular reactions. The systems considered include outer-sphere electron-exchange reactions ($\Delta E = 0$) and outer-sphere electron-transfer reactions accompanied by a net chemical change. The values of E_λ for the latter reactions were calculated from those of the component exchange reactions with the Marcus additivity relation[1,2]

$$(E_\lambda)_{12} = [(E_\lambda)_{11} + (E_\lambda)_{22}]/2 \qquad (13)$$

where $(E_\lambda)_{12}$ is the reorganization parameter for the net reaction and $(E_\lambda)_{11}$ and $(E_\lambda)_{22}$ are the reorganization parameters for the relevant exchange reactions. The nuclear factors again span a very wide range.

Unlike the case of $*Ru(bpy)_3^{2+}$ deactivation, the classical and quantum-mechanical expressions yield values for the nuclear factor for the $*Ru(bpy)_3^{2+}$–$Ru(bpy)_3^{3+}$ reaction (which also lies in the inverted region) that do not differ appreciably. The reason for this small difference is that the classical (solvent) barrier makes a relatively large contribution to E_λ for the bimolecular reaction but not to E_λ for the excited-state decay.[44] The two excited-state processes also differ in another important respect: an additional decay channel is possible for the $*Ru(bpy)_3^{2+}$–$Ru(bpy)_3^{3+}$ reaction. Thus, electronically excited $Ru(bpy)_3^{3+}$ is an accessible product of the bimolecular reaction,[47,48] and ΔE for such a reaction would place this process in the normal free-energy region yielding $\kappa_n \sim 1$. No such channel exists for $*Ru(bpy)_3^{2+}$ deactivation since the state considered is the lowest excited state of the system.

The clearest evidence for the formation of excited products is provided by chemiluminescent reactions. The occurrence of such reactions, in turn, provides support for the validity of the rate decreases in the inverted region. For example, the efficiency of excited-state formation in the reaction

(43) Forster, M.; Hester, R. E. *Chem. Phys. Lett.* **1981**, *81*, 42.

(44) (a) Resonance Raman studies have shown[45] that the electron promoted in the MLCT transition in $Ru(bpy)_3^{2+}$ is located on a single bipyridine ligand rather than delocalized over all three ligands. Despite this, the MLCT absorption and emission bands show very little solvent dependence. A large solvent dependence in symmetrical systems of this type is not expected if the ligand-to-ligand electron hopping frequency is sufficiently high for the charge distribution in the excited state to be essentially spherically symmetrical on the time scale for solvent polarization. This interpretation is supported by the observation that the electron hopping frequency in $Fe(bpy)_3^+$ is $>10^{10}\ s^{-1}$.[46]

(45) Dallinger, R. F.; Woodruff, W. H. *J. Am. Chem. Soc.* **1979**, *101*, 4391.

(46) Motten, A. G.; Hanck, K.; DeArmond, K. *Chem. Phys. Lett.* **1981**, *79*, 541.

(47) Creutz, C.; Sutin, N. *J. Am. Chem. Soc.* **1977**, *99*, 241.

(48) Siders, P.; Marcus, R. A. *J. Am. Chem. Soc.* **1981**, *103*, 748.

$$Ru(bpy)_3^{+} + Ru(bpy)_3^{3+} \rightarrow {}^*Ru(bpy)_3^{2+} + Ru(bpy)_3^{2+} \rightarrow Ru(bpy)_3^{2+} + Ru(bpy)_3^{2+}$$

is near 100% in acetonitrile below 240 K;[49] such a high efficiency for the formation of excited-state products strongly suggests that the reaction to form ground-state products is inhibited by its very large exothermicity (or by a less favorable electronic factor).

The Frequency Factor

It follows from eq 4 that $k_{el} = \nu_n$ when the reaction is barrierless ($\kappa_n = 1$) and the electronic factor for the reaction is unity ($\kappa_{el} = 1$). Under these conditions the activation-controlled rate constant is equal to the frequency factor ($K_A\nu_n$ for a bimolecular reaction and ν_n for a unimolecular reaction). K_A is given by eq 3, and for the present purpose we take $r = \sigma$ and $\delta r = 0.8$ Å; the latter value is typical for electron-transfer reactions involving spherical metal complexes.[19] In the classical model ν_n is the frequency of passage across the barrier, that is, the frequency of the vibration that destroys the activated complex configuration. It is given by[7]

$$\nu_n^2 = \sum \nu_i^2 E_i / \sum E_i \qquad (14)$$

where $\nu_i = (f_i/\mu_i)^{1/2}/2\pi$ is the harmonic frequency of the ith mode (reduced mass μ_i) and $E_i/4$ is its contribution to the barrier. The value of ν_n ranges from $\sim 10^{12}$ s^{-1} to $\sim 10^{14}$ s^{-1} depending on whether the barrier-crossing vibration is predominantly a solvent mode or a high-frequency intramolecular mode. Values of the frequency factors for the systems under discussion are included in Table I.

The Electronic Factor

The splitting that occurs at the intersection of the two potential-energy surfaces (Figure 1) is crucial for the electron transfer. This splitting is equal to $2H_{AB}$, where H_{AB} is the electronic coupling matrix element $\langle\psi_A|H|\psi_B\rangle$.[50] The electronic factor (also called the electronic transmission coefficient)[16] is proportional to H_{AB}^2 and attains a maximum value of unity at sufficiently large H_{AB}. Within the Landau–Zener framework the electronic factor in the high-temperature limit can be expressed as[18,19]

$$\kappa_{el} = \frac{2(1 - \exp(-\nu_{el}/2\nu_n))}{2 - \exp(-\nu_{el}/2\nu_n)} \qquad (15)$$

$$\nu_{el} = \frac{2H_{AB}^2}{h}\left[\frac{\pi^3}{(\Delta G_{out}^* + \Delta G_{in}^*)4RT}\right]^{1/2} \qquad (16)$$

where ν_{el} is an electronic frequency and ν_n is the nuclear frequency introduced earlier. The choice of the form of $\kappa_{el}(r)$ is made here so as to coincide, in the case of the very strong coupling limit,[39] with the usual Landau–Zener probability factor calculated at that r. It is evident from eq 15 that $\kappa_{el} = 1$ when $\nu_{el} >> 2\nu_n$ and that $\kappa_{el} = \nu_{el}/\nu_n$ when $\nu_{el} << 2\nu_n$; thus $k_{el} = \nu_n\kappa_n$ when $\kappa_{el} = 1$ while $k_{el} = \nu_{el}\kappa_n$ when $\kappa_{el} << 1$.

(Reactions for which $\kappa_{el} = 1$ and $<< 1$ are frequently called adiabatic and nonadiabatic, respectively. These designations should be used with caution since they refer only to reactions in the normal free-energy region. Reactions in the inverted region are inherently nonadiabatic: the rate constant for adiabatic electron transfer in the inverted region is zero (unless the energy of the reactants lies above the energy of the interection).)

As we did for the nuclear factor, we consider two low-temperature cases (the same qualifications that were introduced for the nuclear factors also apply here).

(1) $\Delta G_{AB}^\circ \sim 0$. Under these conditions ν_{el} is given by[16,23]

$$\nu_{el} = \frac{2H_{AB}^2}{h} \times \left[\frac{\pi^3}{\left(E_{out} + E_{in}\left(\frac{h\nu_{in}}{2kT}\right)\mathrm{csch}\left(\frac{h\nu_{in}}{2kT}\right)\right)RT}\right]^{1/2} \qquad (17)$$

Note that eq 17 reduces to eq 16 in the high-temperature limit.

(2) $\lambda << -\Delta G_{AB}^\circ$. Under these conditions ν_{el} is given by[24,51]

$$\nu_{el} = \frac{2H_{AB}^2}{h}\left(\frac{2\pi^3}{h\nu_M|\Delta E|}\right)^{1/2} \qquad (18)$$

Like the nuclear factor, ν_{el} *decreases* with increasing energy gap.

Applications. Values of H_{AB} and κ_{el} are presented in Table II. The three spin-equilibrium relaxations,[52] the decay of the LF excited state of $Fe(bpy)_3^{2+}$, and the electron transfer in the $Co(en)_3^{2+}$–$Co(en)_3^{3+}$ exchange reaction[53] are formally spin forbidden. These two-electron processes become allowed through spin–orbit coupling which mixes the wave functions for intermediate spin states with the wave functions for the initial (or final) states:

$$\psi = \psi_1 + c\psi_2 \qquad (19)$$

$$c = \frac{\langle\psi_2|H_{so}|\psi_1\rangle}{E_2 - E_1} \qquad (20)$$

where c is the mixing coefficient, H_{so} is the spin–orbit interaction operator, and E_2 and E_1 are the energies of the intermediate and initial (or final) spin states.

The spin–orbit coupling parameters for the free ions were used to estimate H_{AB} for these systems. The values of H_{AB} for the decay of the MLCT excited state of $Ru(bpy)_3^{2+}$ and for electron transfer in the mixed-valence systems were estimated from the intensities of the charge-transfer bands[30-33] by means of the Mulliken–Hush expressions.[54,55] The H_{AB} values for the $Fe(H_2O)_6^{2+}$–$Fe(H_2O)_6^{3+}$ and $Ru(bpy)_3^{2+}$–$Ru(bpy)_3^{3+}$ exchange reactions were obtained from ab initio calcula-

(49) Wallace, W. L.; Bard, A. J. *J. Phys. Chem.* **1979**, *83*, 1350.
(50) The splitting at the intersection is only equal to $2H_{AB}$ when the overlap of the electronic wave functions can be neglected. More generally it is equal to $2(H_{AB} - S_{AB}H_{AA})/(1 - S_{AB}^2)$ where $S_{AB} = \langle\psi_A|\psi_B\rangle$.
(51) The factorization of the rate constant expression for the weak coupling case is done by analogy with the very strong coupling case; thus eq 18 was chosen so that when multiplied by eq 12 and introduced into eq 15 it gives the Englman–Jortner result for the weak coupling case.
(52) Buhks, E.; Navon, G.; Bixon, M.; Jortner, J. *J. Am. Chem. Soc.* **1980**, *102*, 2918.
(53) Buhks, E.; Bixon, M.; Jortner, J.; Navon, G. *Inorg. Chem.* **1979**, *18*, 2014.
(54) Mulliken, R. S. *J. Am.* Chem. *Soc.* **1952**, *64*, 1811.
(55) Hush, N. S. *Prog. Inorg. Chem.* **1967**, *8*, 357.

Table II
Electronic Factors and Comparison of Calculated and Observed Rate Constants[a]

reaction	$-H_{AB}$, cm^{-1}	κ_{el}	k_{calcd}[e]	k_{obsd}[e]	ref
$FeL_6^{2+}(^1A) \rightleftharpoons FeL_6^{2+}(^5T)$ $(d\pi)^6$ $(d\pi)^4(d\sigma^*)^2$	20-200	$(10^{-3}$-$10^{-1})^b$	10^7-10^9	10^5-10^8	25, 26, 36
$FeL_6^{3+}(^2T) \rightleftharpoons FeL_6^{3+}(^6A)$ $(d\pi)^5$ $(d\pi)^3(d\sigma^*)^2$	20-200	$(10^{-3}$-$10^{-1})^b$	10^7-10^9	10^6-10^7	25, 28, 37
$*Fe(bpy)_3^{2+}(^5T) \rightarrow Fe(bpy)_3^{2+}(^1A)$ $(d\pi)^4(d\sigma^*)^2$ $(d\pi)^6$	20-200	$(10^{-3}$-$10^{-1})^b$	10^9-10^{11}	1×10^9	26
$*Ru(bpy)_3^{2+}(^3(d\text{-}\pi^*)) \rightarrow Ru(bpy)_3^{2+}(^1A)$ $(d\pi)^5(L\pi)^1$ $(d\pi)^6$	~100	$\sim 10^{-2}$	10^{-163}[f] 10^{-1},[g] 10^1[h]	2×10^6 6×10^3[i]	29 64
$(NH_3)_5Ru^{II}(4,4'\text{-bpy})Ru^{III}(NH_3)_5 \rightarrow (NH_3)_5Ru^{III}(4,4'\text{-bpy})Ru^{II}(NH_3)_5$	~400	1.0[a]	10^8[k]		30, 31
$(NH_3)_5Ru^{II}(py)CH_2(py)Ru^{III}(NH_3)_5 \rightarrow (NH_3)_5Ru^{III}(py)CH_2(py)Ru^{II}(NH_3)_5$	~90	0.2[b]	10^5		32, 33
$Co(en)_3^{2+} + Co(en)_3^{3+} \rightarrow Co(en)_3^{3+} + Co(en)_3^{2+}$	5-30	$(10^{-3}$-$10^{-2})^d$	10^{-6}-10^{-5}	8×10^{-5}	65
$Fe(H_2O)_6^{2+} + Fe(H_2O)_6^{3+} \rightarrow Fe(H_2O)_6^{3+} + Fe(H_2O)_6^{2+}$	~30	$\sim 10^{-2}$ [b]	10^{-2}	4	66
$Ru(bpy)_3^{2+} + Ru(bpy)_3^{3+} \rightarrow Ru(bpy)_3^{3+} + Ru(bpy)_3^{2+}$	20-100	$\sim 1^b$	10^9	4×10^8	67
$Fe(H_2O)_6^{2+} + Ru(bpy)_3^{3+} \rightarrow Fe(H_2O)_6^{3+} + Ru(bpy)_3^{2+}$	25-55	$\sim 10^{-1}$ [b]	10^8	5×10^6	68
$*Ru(bpy)_3^{2+} + Ru(bpy)_3^{3+} \rightarrow Ru(bpy)_3^{3+} + Ru(bpy)_3^{2+}$	~100	$\sim 1^c$	10^{-2},[f] 1,[g] 10^{12}[j]	2×10^9	47

[a] Note that ν_n cancels in the product $\nu_n\kappa_{el}$ when $\kappa_{el} << 1$. [b] Calculated by using eq 15 and 16. [c] Calculated by using eq 15 and 18. [d] Calculated by using eq 15 and 17. [e] Units of the rate constants are s^{-1} and M^{-1} s^{-1} for the unimolecular and bimolecular reactions, respectively. Temperature is 25 °C unless otherwise indicated. [f] Calculated from the classical expressions. [g] Calculated from the quantum-mechanical expressions with $E_M = 800$ cm^{-1} and $h\nu_M = 1300$ cm^{-1}. [h] Calculated from the quantum-mechanical expressions with $E_M = 800$ cm^{-1} and $h\nu_M = 1600$ cm^{-1}. [i] This is the value of the nonradiative rate constant at 4.2 K. [j] Calculated from the quantum-mechanical expressions with $E_M = 5300$ cm^{-1} and $h\nu_M = 1300$ cm^{-1}. The calculated rate constant is not corrected for diffusion control. [k] Corrected for lowering of the barrier by H_{AB}.

tions[56] and from computations based upon an approximate model,[57] respectively, while the H_{AB} values for the cross-reactions were obtained from the geometric-mean approximation[58]

$$(H_{AB})_{12} = [(H_{AB})_{11}(H_{AB})_{22}]^{1/2} \quad (21)$$

where the subscripts have the same meanings as in eq 13.

Other measurements that can be used to obtain H_{AB} or κ_{el} include the apparent entropies of activation ($\Delta S_{el}^* = R \ln \kappa_{el}$), and the magnitudes of the rate constants observed in the barrierless region ($k_{lim} = K_A\kappa_{el}\nu_n$ if $K_A\kappa_{el}\nu_n < k_{diff}$). These procedures must be used with caution: the temperature dependence of the electrostatic work required to bring similarly charged reactants together should also make the entropy of activation more negative, and, since $K_A\nu_n \sim 10^{12}$–10^{13} M^{-1} s^{-1} (vide infra), diffusion control may be observed even though $\kappa_{el} \sim 10^{-3}$. Note also that rate saturation below the diffusion-controlled limit may occur for reasons other than $K_A\kappa_{el}\nu_n < k_{diff}$, for example, because of a preequilibrium change on one of the reactants, substitution control, etc.[57]

For many purposes the distance dependence of H_{AB} can be approximated by[59,60]

$$H_{AB} = H_{AB}^\circ \exp[-\beta'(r - \sigma)] \quad (22)$$

where H_{AB}° is the value of H_{AB} when $r = \sigma$. Calculated values of β' range from 1.0 to 2.5 $Å^{-1}$.[4,56,60] Note that $1/2\beta'$ provides an estimate of the lower limit of δr for the reaction.[19]

It is apparent from Table II that the κ_{el} values for the systems considered are in the range 10^{-3}–1, which is a much smaller range than that spanned by the nuclear factors. The lower κ_{el} values are for reactions that are formally spin forbidden. Although none of the electronic factors in Table II is very small, this is not always the case. Thus κ_{el} for the Eu^{2+}_{aq}–Eu^{3+}_{aq} exchange, which involves the shielded f orbitals, is purported to be $<10^{-10}$.[61a] Although this is almost certainly an underestimate, κ_{el} for this system is very probably $<<10^{-3}$.[19b,61b] The electronic coupling decreases with the separation of the redox centers, and it may be very small when large transfer distances are involved, for instance, in certain biological electron transfers[62] or when the electron transfer is between isolated species in rigid media.[63]

On the basis of the *direct* 4d–4d overlap of the two metal centers, the $Ru(bpy)_3^{2+}$–$Ru(bpy)_3^{3+}$ exchange would be highly nonadiabatic at the distance defined by first contact of the bipyridine rings of the two reactants. The κ_{el} value presented in Table II was obtained by estimating the π^*–π^* interaction of the two reactants arising from the delocalization of the metal $d\pi$ electron density onto the π^* orbitals of the bipyridine ligands.[57] Even if considerable interpenetration of the coordination shells of the two reactants

(56) (a) Newton, M. D. *Int. J. Quant. Chem., Symp.* **1980**, *14*, 363. (b) Newton, M. D. *ACS Symp. Ser.* **1982**, *No. 198*, 255.
(57) Creutz, C.; Sutin, N. In "Inorganic Reactions and Methods"; Zuckerman, J. J., Ed.; Springer-Verlag: West Berlin, in press.
(58) Sutin, N. *Acc. Chem. Res.* **1968**, *1*, 225.
(59) Hopfield, J. J. *Proc. Natl. Acad. Sci. U.S.A.* **1974**, *71*, 3640.
(60) Buhks, E.; Jortner, J. *FEBS Lett.* **1980**, *109*, 117.
(61) (a) Balzani, V.; Scandola, F.; Orlandi, G.; Sabbatini, N.; Indelli, M. T. *J. Am. Chem. Soc.* **1981**, *103*, 3370. (b) Instead of a very small electronic factor, a small nuclear factor arising from different hydration numbers of the two oxidation states (larger inner-sphere barrier or small Franck–Condon factor) could be primarily responsible for the relatively slow rates of outer-sphere reactions involving the Eu_{aq}^{3+}–Eu_{aq}^{2+} couple.
(62) Mauk, A. G.; Scott, R. A.; Gray, H. B. *J. Am. Chem. Soc.* **1980**, *102*, 4360.
(63) Miller, J. R.; Beitz, J. V. *J. Chem. Phys.* **1981**, *74*, 6746. Kestner, N. R. *J. Phys. Chem.* **1980**, *84*, 1270.

takes place, it is still likely that the electron transfer in the $Ru(bpy)_3^{2+}$–$Ru(bpy)_3^{3+}$ exchange proceeds predominantly by ligand–ligand overlap. In this connection it is of interest that introducing a methylene group between the pyridine rings of the bipyridine bridging group in the mixed-valence diruthenium system decreases κ_{el} fivefold.

Comparison with Measured Rate Constants

The products of the frequency, electronic, and nuclear factors are compared with the measured rate constants in Table II. Most of the calculated rate constants lie within a factor of 10^2 of the measured values. This level of agreement must be regarded as excellent since even small errors in the estimates of κ_n, κ_{el}, ν_n, and (where relevant) K_A will lead to discrepancies of this order. The least satisfactory agreement is obtained for the $Ru(bpy)_3^{2+}$ excited-state lifetime and for the rate constant for the oxidation of this excited state by $Ru(bpy)_3^{3+}$. Both of these systems are in the inverted region, where the classical models break down. Much better agreement between the calculated and measured rate constants is obtained through the use of the nonclassical eq 12 and 18; the improvement is particularly dramatic for the excited-state lifetime.

In view of the uncertainty in the parameters and the complexity of the excited-state manifold[64] and the approximations in eq 12 and 18, the agreement between the calculated and observed $Ru(bpy)_3^{2+}$ excited-state lifetimes can also be regarded as satisfactory.[69] In the case of the reaction of the excited $Ru(bpy)_3^{2+}$ with $Ru(bpy)_3^{3+}$, the formation of excited $Ru(bpy)_3^{3+}$ could be responsible for the rapid rate since the decrease in ΔE would place the reaction in the normal free-energy region with $\kappa_n \sim 1$. However, there are numerous other bimolecular reactions that do not show inverted behavior where the formation of excited products can be discounted.[47,71-73] It may be significant that good agreement with the observed rates can be obtained by postulating that high-frequency (internal) modes dominate the relaxation even when the contribution of low-frequency (solvent) modes to $\sum E_i$ is substantial.[74,75]

Another explanation for the rapid rates of bimolecular reactions in the inverted region is an increase in E_{out} as a consequence of electron transfer occurring at larger separation distances;[2b] however, recent numerical calculations[76] show this effect to be small. Other possibilities include underestimation of the diffusion-controlled region,[70] rapid relaxation through adiabatic channels in the barrierless region,[77] and a change in reaction mechanism.[78]

Conclusions

The above discussion has shown that the rate constants for spin interconversion, excited-state decay, electron transfer in mixed-valence systems, and bimolecular electron-transfer reactions can be treated in terms of a common formalism in which the rate constants are expressed as a product of a nuclear, an electronic, and a frequency factor. Good agreement with the measured rate constants is obtained in the normal free-energy region. On the other hand, the understanding of electron-transfer rates in the highly exothermic region remains a stimulating challenge to experimentalists and theorists alike.

I thank Drs. C. Creutz, B. S. Brunschwig, N. S. Hush, R. N. Kestner, R. A. Marcus, and M. D. Newton for very helpful discussions. This work was supported by the Office of Basic Energy Sciences of the U. S. Department of Energy.

(64) Elfring, W. H. Jr.; Crosby, G. A. *J. Am. Chem. Soc.* **1981**, *103*, 2683.
(65) Dwyer, F. P.; Sargeson, A. M. *J. Phys. Chem.* **1961**, *65*, 1892.
(66) Silverman, J.; Dodson, R. W. *J. Phys. Chem.* **1952**, *56*, 846.
(67) Young, R. C.; Keene, F. R.; Meyer, T. J. *J. Am. Chem. Soc.* **1977**, *99*, 2468.
(68) Lin, C.-T.; Böttcher, W.; Chou, M.; Creutz, C.; Sutin, N. *J. Am. Chem. Soc.* **1976**, *98*, 6536.
(69) Although the agreement might be improved by mixing in the LF excited state of $Ru(bpy)_3^{2+}$, which lies slightly above the MLCT state, a similar explanation will not hold for $Os(bpy)_3^{2+}$, where the LF state lies well above the MLCT state. The shorter lifetime of $^*Os(bpy)_3^{2+}$ compared to $^*Ru(bpy)_3^{2+}$ is consistent with the smaller energy gap (and larger spin–orbit coupling) for the former system. In terms of the present model, the relatively long lifetime of the LF excited state of $Cr(bpy)_3^{3+}$, for which the Stokes shift is <60 cm^{-1},[70] can be rationalized in terms of the combination of a small electronic factor, resulting from small spin–orbit coupling, and a small nuclear factor, resulting from a small Stokes shift and the absence of an active role for high frequency modes in the metal-centered transition. The absence of a C–H/C–D isotope effect on the lifetime of the $Cr(bpy)_3^{3+}$ excited state is consistent with this interpretation.[26]
(70) Brunschwig, B.; Sutin, N. *J. Am. Chem. Soc.* **1981**, *13*, 865.
(71) Ballardini, R.; Varani, G.; Indelli, M. T.; Scandola, F.; Balzani, V. *J. Am. Chem. Soc.* **1978**, *100*, 7219.
(72) Nagle, J. K.; Dressick, W. J.; Meyer, T. J. *J. Am. Chem. Soc.* **1979**, *101*, 3993.
(73) Bock, C. R.; Connor, J. A.; Gutierrez, A. R.; Meyer, T. J.; Whitten, D. G.; Sullivan, B. P.; Nagle, J. K. *J. Am. Chem. Soc.* **1979**, *101*, 4815. Bock, C. R.; connor, J. A.; Gutierrez, A. R.; Meyer, T. J.; Whitten, D. G.; Sullivan, B. P.; Nagle, J. K. *Chem. Phys. Lett.* **1979**, *61*, 522.

(74) When $E_{out} > |\Delta E_o|$ and a single internal mode of frequency ν_{in} is considered, the following expression for the electron-transfer rate constant at low temperature or low values of $E_{in}/h\nu_{in}$ (normal free-energy region, classical solvent) is obtained by using perturbation theory[24d]

$$k_{el} = \frac{2H_{AB}^2}{h}\left(\frac{\pi^3}{E_{out}RT}\right)^{1/2}\exp\left(-\frac{(E_{out}+\Delta E_o)^2}{4E_{out}RT} - \frac{E_{in}}{h\nu_{in}}\right)$$

In this limit the largest contribution to the rate constant comes from a zero–zero transition of the internal mode, that is, the internal mode transition occurs from the lowest vibrational level of the initial state to the lowest vibrational level of the final state. Under these conditions the driving force for the solvent configuration change is the entire ΔE_o and the exponential dependence of the rate constant on the second power of ΔE_o required by classical theory is once more predicted. On the other hand, when $|\Delta E_o| > E_{in} + E_{out}$ (inverted free-energy region, classical solvent), instead of being given by the exponential in the above expression, the nuclear factor is given by[24d]

$$\exp\left[\left(\frac{E_{out}kT}{h^2\nu_{in}^2}\right)\ln^2\left(\frac{|\Delta E_o| - E_{out}}{E_{in}}\right)\right] \times \left[\exp\left[-\left(\frac{|\Delta E_o| - E_{out}}{h\nu_{in}}\right)\left(\ln\left(\frac{|\Delta E_o| - E_{out}}{E_{in}}\right) - 1\right) - \frac{E_{in}}{h\nu_{in}}\right]\right]$$

which reduces to eq 12 when $E_{out} \to 0$. Note that the dominant low-temperature internal mode transition in the inverted free-energy region is $0 \to v \sim (|\Delta E_o| - E_{out})/h\nu_{in}$ rather than $0 \to 0$. The latter is the case in the normal free-energy region.

(75) The agreement may be further improved by the use of expressions in which anharmonicity and frequency changes are explicitly taken into account.

(76) Marcus, R. A.; Siders, P. *J. Phys. Chem.* **1982**, *86*, 622.
(77) Hush, N. S. In "Mixed-Valence Compounds"; Brown, D. B., Ed.; Reidel: Dordrecht, 1980; p 151.

(78) Rate decreases are not predicted for reactions that proceed by an atom-transfer mechanism. See, for example: Marcus, R. A. *J. Phys. Chem.* **1968**, *72*, 891.